Transactions of the Japan Institute of Metals, Vol. 29, No. 7 (1988), pp. 573 to 579

A Fracture Resistance Measurement Procedure for Brittle Materials

By M. Jenkins*, J. Mikami*, T. Chang* and A. Okura*

A procedure has been developed to measure the fracture resistances of nominally brittle materials (monolithics and composites) using chevron-notched, three-point bend specimens at room temperature and elevated temperatures. The chevron-notched geometry promotes stable crack growth during quasi-static fracture tests. For each test a continuous record of load versus crack mouth opening displacement (CMOD) is obtained. The fracture toughness, work-of-fracture and the classical crack growth resistance curves are then determined from the stable crack growth loading curves and previously established relations between the CMOD compliance, the effective crack length, and the load point displacement (LPD).

Various materials have been tested which include monolithic ceramics: alpha silicon carbide, reaction bonded silicon nitride, and magnesium aluminate spinel and composites: titanium diboride particle/silicon carbide matrix, silicon carbide whisker/aluminium oxide matrix, and carbon fibre/carbon matrix. The R-curves for the various materials show flat, rising linear, and rising non-linear behavior indicative of linear elastic fracture behavior, constant but increasing fracture mechanisms, and constantly developing fracture mechanisms, respectively.

(Received October 30, 1987)

Keywords: *fracture toughness, work-of-fracture, carbon/carbon composites, heat engine component*

I. Introduction

Fracture mechanics is an increasingly important design tool in many areas of advanced technology. However, despite the increasing sophistication of the numerical and analytical techniques employing fracture mechanics, the successful application of these methods to a particular problem is still limited by the knowledge of the design material's fracture characteristics. The acquisition of reliable data on material fracture characteristics is dependent on the integrity of the fracture testing procedure.

The American Society for Testing and Materials (ASTM) has adopted two test standards for evaluating the linear elastic fracture characteristics of materials. The validity of both these standards; one for determining the plane strain fracture toughness[1] and the other for determining the crack growth resistance[2]; is restricted to metals at room temperature.

The recent growing interest in ceramic materials (monolithic and composite) has created a need to establish a standardized procedure for fracture testing these nominally brittle materials at both room temperature and at the elevated temperatures where many of the applications of these materials lie[3][4].

This paper presents a procedure, shown schematically in Fig. 1, for testing nominally brittle materials at both room temperature and elevated temperatures. The chevron-notched, three-point bend specimen is discussed and the compliance technique for continuously monitoring effective crack length is presented. A highly sensitive laser interferometric strain gage (LISG) is described for measuring the specimen compliances independently of the temperature and load-dependent machine compliances. Finally, the techniques for determining fracture resistance are discussed and the test results are presented for various types of monolithic and composite materials.

* Institute of Industrial Science, The University of Tokyo, 7-22-1 Roppongi, Minato-ku, Tokyo 106, Japan.

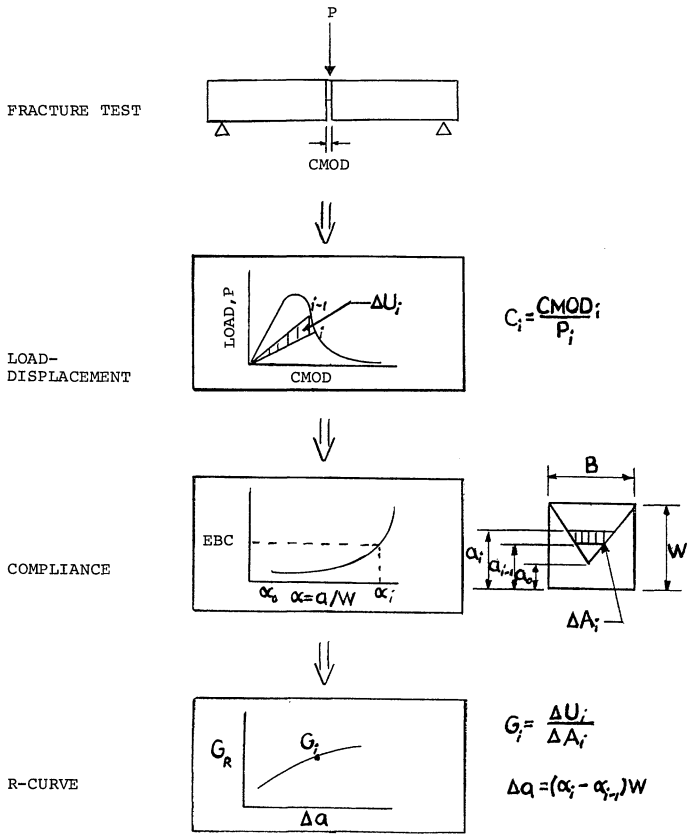

Fig. 1 Schematic diagram of the procedure to measure fracture resistance.

II. Chevron-Notched Test Specimen

Many types of specimen geometries have been used for fracture testing brittle materials. The more popular geometries include the double-torsion beam specimen[5], the wedge-loaded-double-cantilever-beam specimen[6], and the single-edge-notched bend bar[7].

The single-edge-notched bend bar provides the advantages of ease of machining both the specimen and the notch, the need for a minimum amount of material to produce the specimen, and the simply applied compressive loads at the reaction points. The three-point loading arrangement used in this study is the simplest loading situation. This is an important consideration at elevated temperatures where the complications of the four-point loading apparatus may produce unquantifiable eccentric loading.

The chevron-notch geometry holds two distinct advantages over the traditional straight-through notch when fracture testing brittle materials[8]-[12]. The first advantage is that a 'real' starter crack (necessary for determining 'true' fracture parameters) is automatically initiated at a low load due to the high stress concentration at the chevron tip. The second advantage is that the crack is forced to propagate in a stable manner due to the ever-increasing crack front over the duration of the chevron section. This allows the complete study of stable crack growth from one specimen even in a brittle material. Comparisons are shown in Fig. 2 for the chevron-notched and the traditional straight-notched, three-point bend specimens.

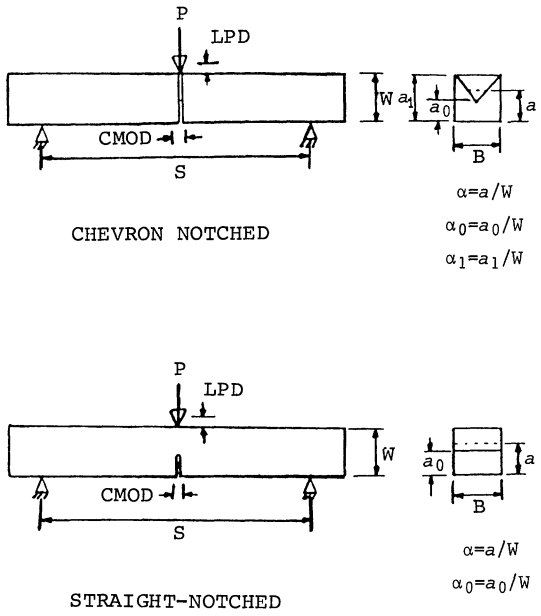

Fig. 2 Comparison of chevron- and straight-notched three-point bend specimens.

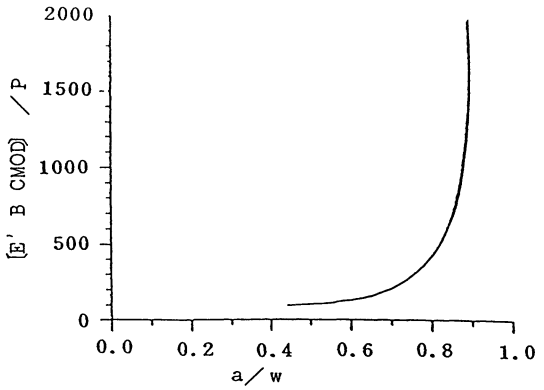

Fig. 3(a) Dimensionless compliance curve for a chevron-notched, three-point bend specimen, $\alpha_0=0.44$.

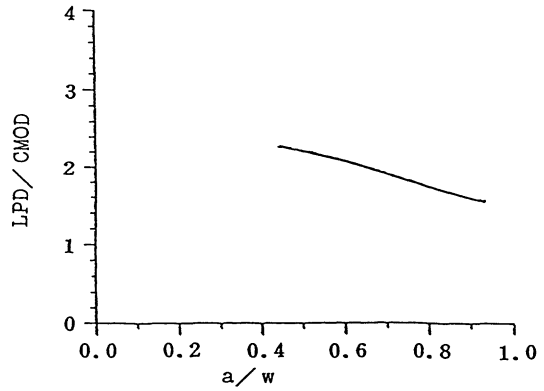

Fig. 3(b) LPD/CMOD relation for a chevron-notched, three-point bend specimen, $\alpha_0=0.44$.

III. Compliance Technique

Crack length must be continuously monitored during stable crack growth in order to determine the crack growth resistance of the material. Three methods are popularly used to do this: the compliance technique[1][2], the visual observation of crack[1][2], and the electric potential drop arrangement[13].

Of these, the compliance technique (where compliance is defined as displacement divided by load) is the simplest and the most workable method for determining the crack extension under a range of temperatures and conditions. A restriction in this technique is that an effective crack length, rather than the actual crack length, is determined using linear elastic assumptions.

Briefly, the compliance technique involves measuring the specimen compliance independently of load fixture compliance. For notched, three-point bend specimens, the crack mouth opening displacement (CMOD), which is normal to the loading direction, and the load are recorded continuously during the stable crack growth fracture test. The effective crack length and fracture parameters are then calculated using a priori relationships between the CMOD compliance and the crack length, and between the CMOD and the load point displacement (LPD). These dimensionless relationships are determined from linear elastic numerical models for each geometry, examples of which are shown in Fig. 3 for a chevron-notched, three-point bend specimen with $a_0/W=0.44$.

IV. CMOD Compliance

The accurate determination of the effective crack length using the compliance technique requires the accurate measurement of the applied load and the CMOD. The applied load may be measured in any environment or condition using a remote load cell and a push rod exten-

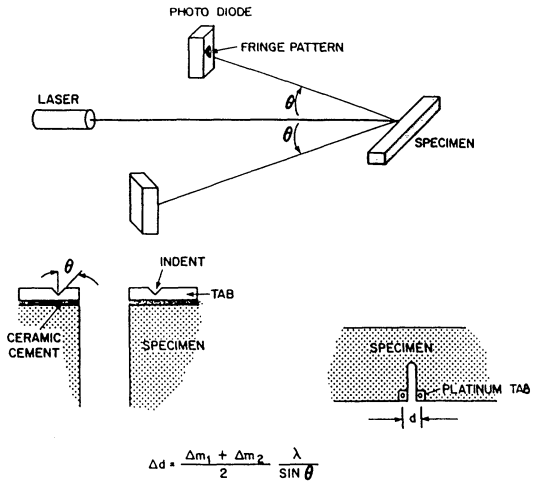

Fig. 4 Schematic view of the LISG test set-up.

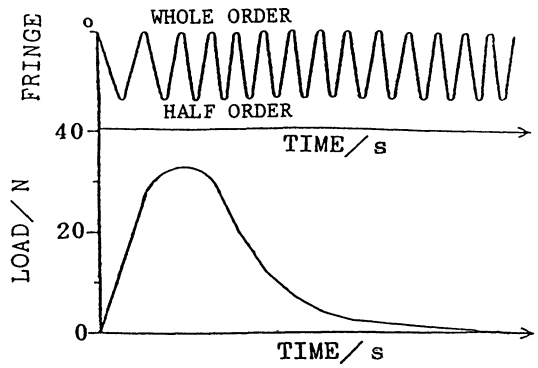

Fig. 5(a) Load and LISG traces.

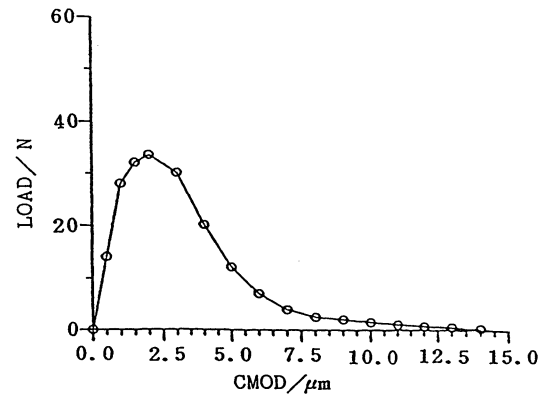

Fig. 5(b) Load versus CMOD curve.

sion. However, the CMOD is not so easily obtained for all conditions.

At room temperature ASTM[1][2] recommends the use of a mechanical clip gage. At elevated temperatures, this type of arrangement is modified by adding long temperature-resistant extensometer arms to isolate the sensing unit from the harsh environment[14]. However these types of mechanical clip gages are of limited use when dealing with either the small displacements (10–15 μm) is materials which are sensitive to extraneous, unquantifiable loads, or small specimens which present limited attachment points for the clip gage.

Because of these limitations, a non-contacting technique has been developed to measure these small displacements at elevated temperatures[15]. The technique, know as a laser interferometric strain gage (LISG) has been successfully applied to the fracture testing of ceramics and ceramic composites[12][16] and is briefly described as follows.

The LISG set-up consists of a 10 mW HeNe laser, two photo diode circuits, and the associated photo diode circuitry as shown schematically in Fig. 4. Interference fringes are generated by the laser beams reflected from Vickers indentations in two platinum tabs which are bonded to the specimen notch mouth opening with a ceramic adhesive[16]. The movement of each whole order interference fringe represents approximately 1.0 μm of CMOD with a resolution of 0.25 μm according to the equation in Fig. 4. Fringe motion together with the applied load are plotted simultaneously on a chart recorder for the duration of the fracture test, as shown in Fig. 5. This record is later reduced to provide a plot of load versus CMOD for the final data reduction.

Obviously, elevated temperature applications of the LISG require a custom-designed test furnace to accommodate the optics of the LISG. However, the modifications to existing furnace designs is not extensive and are easily implemented[12].

V. Data Reduction Techniques

The unprocessed data for each fracture test consists of a plot of load versus CMOD. From

this plot and knowledge of the specimen geometry, three fracture parameters are calculated: fracture toughness, work-of-fracture, and crack growth resistance.

1. Fracture toughness

The calculated fracture toughness is an estimate of the critical stress intensity factor at crack initiation. The apparent fracture toughness for chevron-notched specimens of linear-elastic materials is calculated from the maximum load and the minimum geometry correction factor for the stress intensity factor as proposed by Pook[17] and verified by Munz *et al.*[18] such that:

$$K_{IC} = Y_{min} P_{max} / (BW^{1/2}) \quad (1)$$

where K_{IC} is the fracture toughness, Y_{min} is the minimum geometry correction factor for the stress intensity factor, P_{max} is the maximum load, B is the specimen thickness, and W is the specimen width. The geometry correction factor, Y, for the chevron-notched, three-point bend specimen was reported by Jenkins *et al.*[11]

2. Work-of-Fracture

The work-of-fracture is the average energy consumed by all the fracture mechanisms within a material manifested during stable crack growth. The work-of-fracture is determined from the area under the load versus load point displacement curve divided by twice the total area of one fracture face as shown schematically in Fig. 6 after Nakayama[20] and Tattersall and Tappin[20]. Relationships between the LPD and the CMOD from Jenkins *et al.*[11] are used to determine the load versus LPD curves for the calculation of the work-of-fracture for the chevron-notched specimens.

3. Crack Growth Resistance

The crack growth resistance (R-curve) is a measurement of the fracture resistance as a function of crack extension and is an estimate of the inherent damage tolerance of the material. The R-curves are developed from the stable crack growth plots of load versus CMOD, the CMOD compliance relations[11], and the LPD/CMOD relations[11] such that[21]:

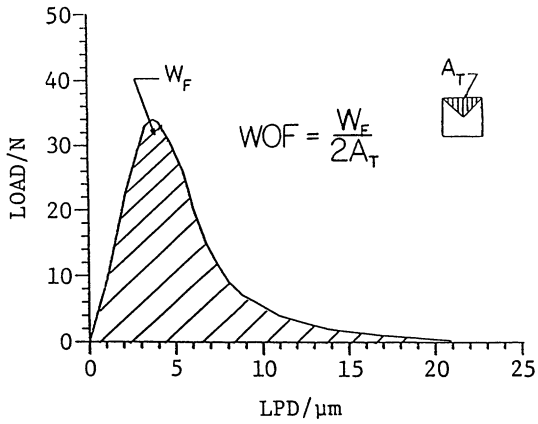

Fig. 6 Diagram of the calculation of work-of-fracture.

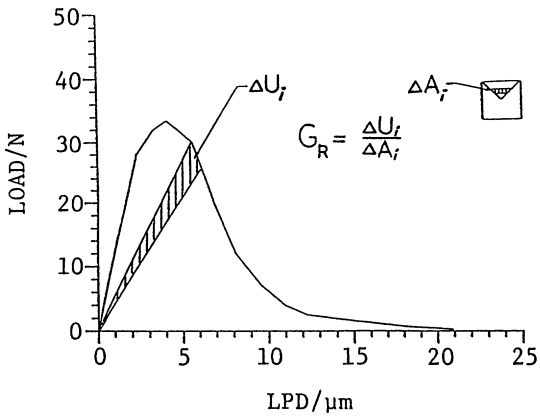

Fig. 7 Diagram of the calculation of the strain energy release rate, G.

$$G_R = \Delta U / \Delta A \quad (2)$$

where G_R is the strain energy release rate, ΔU is the change in the total stored strain energy, and ΔA is the incremental change in fractured area as shown schematically in Fig. 7. The G_R value for a particular crack length is then plotted versus the crack extension from the point of crack initiation.

Similarly the crack growth resistance may also be plotted as the stress intensity factor as a function of incremental crack extension such that[2]

$$K_R = Y_i P_i / (BW^{1/2}) \quad (3)$$

where K_R is the stress intensity factor, Y_i is the instantaneous geometry correction factor for the stress intensity factor calculated for the cor-

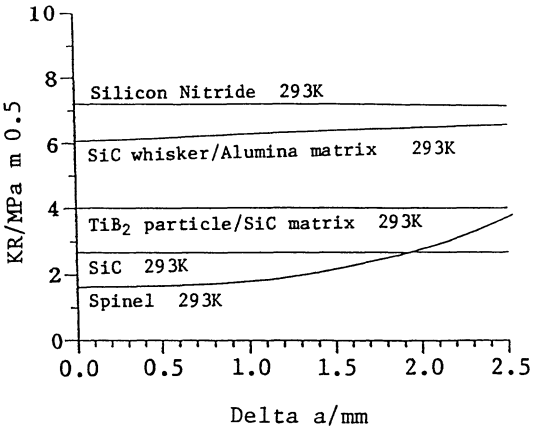

Fig. 8 R-curves for various materials at 293 K.

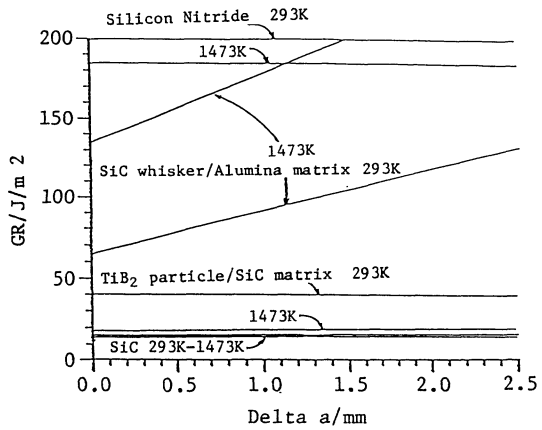

Fig. 9 R-curves for various materials at two temperatures.

responding effective crack length, P_i is the corresponding applied load, and B and W are as defined earlier.

VI. Results

R-curves[12] for various materials at room temperature are shown in Fig. 8. A monolithic alpha silicon carbide shows flat R-curve behavior characteristic of brittle, linear-elastic materials. A rising, linear R-curve is shown for the SiC whisker/alumina matrix composite thus demonstrating the wake fracture process zone of the SiC whiskers. Finally, rising nonlinear R-curves are shown by a monolithic magnesium aluminate spinel and a carbon fibre/carbon matrix composite which the exhibit the 'toughening' effects of multiple fracture process zones (elastic, frontal, wake).

Table 1 Fracture toughness and work-of-fracture for various materials.

Material/ Temperature, K(°C)	Average K_{IC} (MPa $m^{1/2}$)	Average work-of-fracture (J/m^2)
Alpha silicon carbide[22]		
293 (20)	2.91+/−0.31	8.81+/−0.64
1473(1200)	3.37+/−0.05	6.33+/−1.69
R B silicon nitride[23]		
293	6.85+/−0.05	96.7+/−6.94
1473	5.17+/−0.06	76.1+/−10.6
Magnesium aluminate spinel[24]		
293	1.73+/−0.12	6.14+/−1.40
1473	1.00+/−0.12	7.51+/−1.21
SiC whisker/ Alumina matrix[25]		
293	6.56+/−0.19	53.7+/−2.70
1473	5.03+/−0.20	145+/−23.6
TiB_2 particle/ SiC matrix[26]		
293	4.07+/−0.17	19.2+/−1.49
1473	2.81+/−0.11	7.26+/−0.07
Carbon fibre/ Carbon matrix		
293	9.05+/−1.15	4279+/−734

(Average % standard deviation)
(Chevron-notched, three-point bend specimens)
(Ambient air)

R-curves are shown in Fig. 9 for increasing temperatures. The change in the fracture behavior of this material is an important consideration in elevated temperature design applications.

Table 1[12] lists fracture toughness and work-of-fracture values for several materials. Obviously, the present test procedure is readily applicable to a wide range of materials (monolithic and composite) under a variety of temperature conditions.

VII. Conclusions

The conclusions of this study may be summarized as follows.

(1) Fracture resistance may be determined

for various materials using compliance techniques and numerical relations.

(2) Chevron-notched, three-point bend specimens offer a reliable and reproducible means for initiating and maintaining stable crack growth in brittle and semi-brittle materials.

(3) The laser interferometric strain gage provides a simple and inexpensive yet highly accurate, non-contacting means for measuring specimen compliances at elevated temperatures.

(4) The overall test procedure works well for characterizing the fracture resistance of a range of materials under a variety of test temperatures.

REFERENCES

(1) American Society for Testing and Materials, ASTM E 399-83, Philadelphia, Pennsylvania 1983.

(2) American Society for Testing and Materials, ASTM E561-81, Philadelphia, Pennsylvania, 1983.

(3) P. N. Katz: *Nitrogen Ceramics*, F. L. Riley, Ed., Nordoff, Leyden, (1977), p. 643.

(4) D. J. Godfrey: *Proceedings of the British Ceramic Society*, No. 22, (1973), p. 387.

(5) E. R. Fuller, Jr.: *Fracture Mechanics Applied to Brittle Materials*, ASTM STP 678, S. W. Frieman, Eds., American Society for Testing and Materials, (1979), p. 3.

(6) A. S. Kobayashi, A. F. Emery and B. M. Liaw: Amer. Cer. Soc. **66** (1983), 151.

(7) L. A. Simpson: Amer. Cer. Soc. **57** (1974), 151.

(8) J. C. Newman, Jr.: *Chevron-Notched Specimens: Testing and Stress Analysis*, ASTM STP 855, J. H. Underwood, S. W. Frieman, F. I. Baratta, Eds., American Society for Testing and Materials, (1984), p. 5.

(9) D. Munz, R. T. Bubsey and J. L. Shannon, Jr.: J. Amer. Cer. Soc., **63** (1980), 300.

(10) J. A. Salem and J. L. Shannon, Jr.: NASA Technical Memorandum, 87153, 1985.

(11) M. G. Jenkins, A. S. Kobayashi, K. W. White and R. C. Bradt,: to be published in the International Journal of Fracture.

(12) M. G. Jenkins: PhD Dissertation, University of Washington, Seattle, Washington, 1987.

(13) T. B. Troczynski and P. S. Nicholson: Amer. Cer. Soc. Bulletin, **65** (1986), 772.

(14) D. T. Schmale and R. W. Cross,: NUREG/CR-2793, Sandia National Laboratory, Albuquerque, NM, June 1982.

(15) W. N. Sharpe, Jr.: *Handbook on Experimental Mechanics*, A. S. Kobayashi, Ed., Society for Experimental Mechanics, Chapter 13, (1987).

(16) M. G. Jenkins, A. S. Kobayashi, M. Sakai, K. W. White and R. C. Bradt: submitted to The Amer. Cer. Soc. Bulletin, June 1986.

(17) L. P. Pook: International Journal of Fracture Mechanics, **8** (1972), 103.

(18) D. G. Munz, J. L. Shannon, Jr. and R. T. Bubsey: International Journal of Fracture, **16** (1980), R137.

(19) J. Nakayama: Jap. J. Appl. Phys. **3** (1964), 422.

(20) H. G. Tattersall and G. Tappin: Mater. Sci. **1** (1966), 296.

(21) K. Hellan: *Introduction to Fracture Mechanics*, McGraw-Hill, New York, (1984), p. 53.

(22) Hexoloy SA, Standard Oil Engineered Materials Co, Niagara Falls, New York, USA.

(23) A2Y6, GTE Sylvania, Towanda, Pennsylvania, USA.

(24) Coors Porcelain Co., Boulder, Colorado, USA.

(25) HA9S, ARCO Advanced Materials Division, Greer, South Carolina, USA.

(26) Hexoloy ST, Standard Oil Engineered Materials, Co, Niagara Falls, New York, USA.